Identification and characterization of naturally occurring DSF-family quorum sensing signal turnover system in the phytopathogen *Xanthomonas*

Lian Zhou,[1][†] Xing-Yu Wang,[1][†] Shuang Sun,[1]
Li-Chao Yang,[2] Bo-Le Jiang[2] and Ya-Wen He[1]*

[1]*State Key Laboratory of Microbial Metabolism, Joint International Research Laboratory of Metabolic & Developmental Sciences, School of Life Sciences & Biotechnology, Shanghai Jiao Tong University, Shanghai 200240, China.*
[2]*State Key Laboratory for Conservation and Utilization of Subtropical Agro-Bioresources, College of Life Science and Technology, Guangxi University, Nanning 530004, China.*

Summary

Molecules of the diffusible signal factor (DSF)-family are a class of quorum sensing (QS) signals used by the phytopathogens *Xanthomonas*. Studies during the last decade have outlined how *Xanthomonas* cells enter the QS phase. However, information on the mechanism underlying its exit from the QS phase is limited. RpfB has recently been reported as a fatty acyl-CoA ligase (FCL) that activates a wide range of fatty acids to their CoA esters *in vitro*. Here, we establish an improved quantification assay for DSF-family signals using liquid chromatography-mass spectrometry in *X. campestris* pv. *campestris* (*Xcc*). We first demonstrated that RpfB represents a naturally occurring DSF-family signal turnover system. RpfB effectively turns over DSF-family signals DSF and BDSF *in vivo*. RpfB FCL enzymatic activity is required for DSF and BDSF turnover. Deletion of *rpfB* slightly increased *Xcc* virulence in the Chinese radish and overexpression of *rpfB* significantly decreased virulence. We further showed that the expression of *rpfB* is growth phase-dependent, and its expression is significantly enhanced when *Xcc* cells enter the stationary phase. DSF regulates *rpfB* expression in a concentration-dependent manner. *rpfB* expression is also negatively regulated by the DSF signalling

components RpfC, RpfG and Clp. The global transcription factor Clp directly binds to the AATGC-tgctgc-GCATC motif in the promoter region of *rpfB* to repress its expression. Finally, RpfB-dependent signal turnover system was detected in a wide range of bacterial species, suggesting that it is a conserved mechanism.

Introduction

It has been widely accepted that bacterial cells are capable of sensing and responding to changes in their population by communicating with small signal molecules, a mechanism known as quorum sensing (QS). Over the past two decades, research has not only identified a range of QS signals, but has also unveiled unique QS signalling pathways and mechanisms (Deng *et al.*, 2011; Rutherford and Bassler, 2012; Yong and Zhong, 2013). These findings have outlined how bacterial cells enter the QS phase. However, the mechanism underlying how bacterial cells exit the QS phase remains elusive. Accumulating evidence suggests that signal turnover is one of the most important ways for bacterial cells to exit the QS phase (Dong *et al.*, 2007). Acyl homoserine lactone (AHL) is a class of well-studied QS signals produced by more than 80 Gram-negative bacterial species. A range of AHL signal degradative enzymes, such as lactonases and acylases, have been characterized in bacteria and mammals (Zhang *et al.*, 2002; Draganov *et al.*, 2005). Most of these enzymes are derived from non-AHL producing bacterial species, suggesting that they might have significant implications among microorganisms in competing for nutrients and ecological niches (Dong *et al.*, 2007). At least two AHL-dependent QS bacterial species, *Agrobacterium tumefaciens* and *Pseudomonas aeruginosa*, carry naturally occurring QS signal degradation enzymes (Zhang *et al.*, 2002; Sio *et al.*, 2006; Wahjudi *et al.*, 2011). In *Agrobacterium tumefaciens*, a lactonase-like enzyme, AttM, was induced at the stationary phase to turn over the 3OC8HSL signal to regulate Ti plasmid conjugal transfer (Zhang *et al.*, 2002; Lang and Faure, 2014). Although signal turnover is a common mechanism in different QS systems, the genetic components of these systems in most bacterial species have yet to be identified.

Diffusible signal factor (DSF)-family signals represent a class of QS signals with the *cis*-2-unsaturated fatty acid moiety in Gram-negative bacterial pathogens (He and Zhang, 2008; Deng *et al.*, 2011; Ryan and Dow, 2011). *Xanthomonas campestris* pv. *campestris* (*Xcc*), the causal agent of black rot in crucifers, has been used as the model system in studying the mechanism underlying DSF signalling. In *Xcc*, the production, perception and response to DSF-family signals require products of the regulation of pathogenicity factors (*rpf*) gene cluster. RpfF, a key DSF biosynthase with both acyl-ACP thioesterase and dehydratase activity, is required for the synthesis of DSF-family signals DSF, BDSF and CDSF (Barber *et al.*, 1997; Bi *et al.*, 2012). The two-component system comprising the sensor kinase RpfC and the response regulator RpfG has been implicated in DSF perception and signal transduction. RpfC is a dual-function protein that uses a conserved phosphorelay mechanism to transduce the DSF-family signal to its cognate downstream signalling component RpfG to modulate virulence factor production, and meanwhile negatively controls DSF-family signal production through a specific protein–protein interaction with RpfF (Slater *et al.*, 2000; He *et al.*, 2006a). The HD-GYP domain of RpfG is a phosphodiesterase that is activated by the DSF signalling system to perform its regulatory activity by enzymatic degradation of intracellular second messenger cyclic-di-GMP (Ryan *et al.*, 2006). The HD-GYP domain also forms a dynamic complex with GGDEF and PilZ domain proteins such as XC_0420 and XC_0249 to regulate virulence and motility (Ryan *et al.*, 2010; 2012). Clp, the global transcription factor and a key component of the DSF regulatory network, is an effector of c-di-GMP (Chin *et al.*, 2010; Tao *et al.*, 2010). Clp regulates the transcriptional expression of various genes through a hierarchical signalling network in *Xcc* (He *et al.*, 2007). Several bacterial strains belonging to genera *Bacillus*, *Paenibacillus*, *Microbacterium*, *Staphylococcus* and *Pseudomonas* are capable of rapidly breaking down DSF (Newman *et al.*, 2008). *carAB*, which is required for the synthesis of carbamoylphosphate, was further characterized to rapidly degrade DSF in *Pseudomonas* spp. (Newman *et al.*, 2008). However, little is known of the naturally occurring DSF signal turnover system in *Xcc*.

The *rpfB* gene is located immediately upstream of *rpfF* within the *rpf* gene cluster and was initially suggested to be required for DSF biosynthesis, together with *rpfF* in *Xcc* (Barber *et al.*, 1997). A subsequent study showed that RpfB is absolutely not required for DSF synthesis, and mutations in *Xcc*-disrupting *rpfB* apparently have a polar effect on the downstream *rpfF* (Almeida *et al.*, 2012). RpfB has been shown to be involved in DSF processing in both *Xylella fastidiosa* and *Xcc*, affecting the profile of DSF-like fatty acids as observed in thin-layer chromatography (Almeida *et al.*, 2012). A recent study unveiled that

RpfB functions as a fatty acyl-CoA ligase (FCL) that plays a role in fatty acid β-oxidation to give acyl-CoAs for membrane lipid synthesis in *Xcc*. It also plays a more important role in pathogenesis by counteracting the thioesterase activity of DSF synthase RpfF (Bi *et al.*, 2014). Although RpfB utilizes different fatty acids of variable chain lengths, *in vitro* enzymatic activity assays have shown that RpfB apparently has little effect on the QS signals DSF and BDSF (Bi *et al.*, 2014).

In the present study, we demonstrated that RpfB represents a naturally occurring DSF-family QS signals turnover system, which contributes to *Xcc* virulence in Chinese radish. RpfB expression is repressed by the DSF signalling cascade and the global transcription regulator Clp. The RpfB-dependent signal turnover system is present in a wide range of bacterial species, suggesting that it is a conserved mechanism for bacterial cells to exit from the QS mode.

Results

An improved assay for DSF, BDSF and sodium oleate using liquid chromatography-mass spectrometry (LC-MS) or gas chromatography-mass spectrometry (GC-MS)

In the present study, to determine the levels of DSF-family signals in *Xcc* culture during the growth, a LC-MS-based DSF quantification assay was established using the standard DSF and BDSF (Fig. S1). In this method, 0.2 ml of the supernatant from Δ*rpfC* cultures or 20 ml of the supernatant from wild-type cultures are used for DSF and BDSF extraction by ethyl acetate as described in the *Experimental procedures*. The ethyl acetate extract was evaporated and dissolved in 100 µl of methanol as a crude extract. Three microlitres of the crude extract were loaded for DSF and BDSF analysis by LC-MS (Fig. S1). According to this method, the DSF levels in the supernatant of wild-type strains XC1 ranged from 0.002 µM to 0.113 µM, whereas that of BDSF ranged from 0.001 µM to 0.030 µM during the growth (Fig. 1). The DSF levels in the supernatant of the Δ*rpfC* strain ranged from 0.55 µM to 6.00 µM, whereas BDSF levels ranged from 0.15 µM to 1.14 µM, respectively, during the growth (Fig. S2). In the present study, sodium oleate was used as a control for the RpfB FCL activity assay. To monitor the levels of sodium oleate in the supernatant, a GC-MS-based DSF quantification assay was also established using the standard sodium oleate as described in the *Experimental procedures* and in Fig. S3.

RpfB is responsible for BDSF and DSF turnover in *Xcc*

In the present study, we first repeated the *in vitro* assay as previously described (Bi *et al.*, 2014) to test the FCL activ-
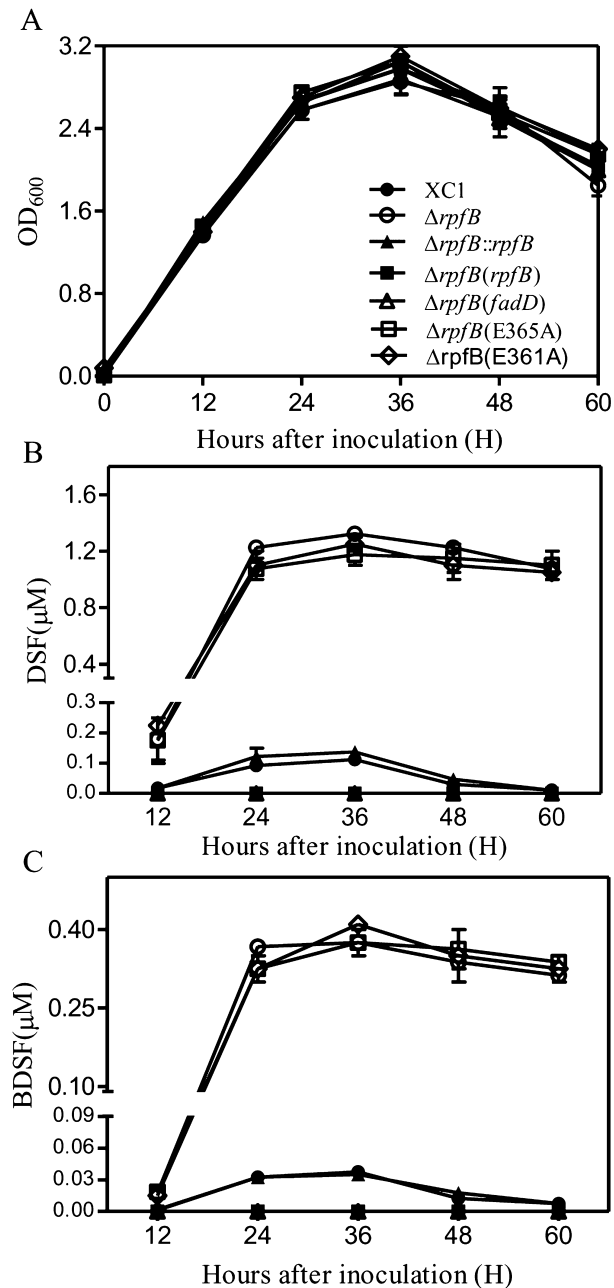
Fig. 1. Time-course of DSF and BDSF production in *Xcc* strains. (A) Time-course of bacterial growth in NA liquid medium, (B) DSF production and (C) BDSF production. Δ*rpfB*(E365A) indicates the *rpfB* deletion mutant overexpressing RpfB with a point mutation at Glu[365] via the expression vector pLAFR3. Δ*rpfB*(E361A) indicates the *rpfB* mutant overexpressing FadD with a point mutation at Glu[361]. Data are expressed as the means ± one standard deviation of three independent assays.

ity of RpfB. The levels of DSF or BDSF decreased only by about 15% after 5 h of incubation at 37°C (Fig. S4), whereas 97.4% of sodium oleate was converted under the same conditions (Fig. S5). These results confirmed that RpfB has a very low activity towards BDSF and DSF.

Since it can be argued that *in vitro* results are often of questionable relevance to an *in vivo* situation, we attempted to assess the *in vivo* activity of RpfB in *Xcc*. We generated *rpfB* deletion or overexpression strains and determined the DSF and BDSF production in its culture supernatant. Two major QS signals, DSF and BDSF, with DSF being the predominant signal during the growth in NA liquid medium, were detected in the supernatants of the *Xcc* strains (Fig. 1). The maximum production of DSF and BDSF in the supernatant of the wild-type strain XC1 was observed at 24–36 h after inoculation; both signals were very low at 60 h after inoculation (Fig. 1B and C). Deletion of *rpfB* (Δ*rpfB* hereafter) resulted in about a 10.0-fold increase in DSF and BDSF production compared with that of the parent strain XC1 at 36 h after inoculation (Fig. 1B and C). Complementation with a single copy of *rpfB* (hereafter Δ*rpfB*::*rpfB*) fully restored DSF and BDSF production to that of the wild-type levels. Overexpression of *rpfB* in the strain Δ*rpfB* [Δ*rpfB*(*rpfB*) hereafter] abolished DSF and BDSF production (Fig. 1B and C).

Deletion and overexpression of *rpfB* were also conducted in the DSF-overproducing strain Δ*rpfC*. The levels of DSF and BDSF produced by strain Δ*rpfB*Δ*rpfC* increased by about 8.8-fold and 6.7-fold, respectively, over the parent strain Δ*rpfC* at 36 h after inoculation (Fig. S2). Complementation with a single copy of *rpfB* fully restored DSF and BDSF production to that of the Δ*rpfC* level. Overexpression of *rpfB* abolished DSF and BDSF production (Fig. S2).

Since DSF and BDSF are synthesized inside the *Xcc* cells, and are then secreted from the cells, cellular DSF and BDSF from three *Xcc* strains, i.e. Δ*rpfC*, Δ*rpfC*Δ*rpfB* and Δ*rpfC*Δ*rpfB*::*rpfB*, were also extracted and determined as described in the *Experimental procedures*. The results showed that deletion of *rpfB* significantly increased cellular DSF and BDSF production (Fig. 2). Overexpression of *rpfB* dramatically reduced cellular DSF and BDSF production (Fig. 2).

To further test the signal turnover activity in RpfB, DSF and BDSF were added to fresh NA cultures ($OD_{600} = 0.5$) of XC1, Δ*rpfB* and Δ*rpfB*(*rpfB*) at a final concentration of 15.0 μM and 8.0 μM respectively. After incubation for 1–3 h, DSF and BDSF in the supernatant were extracted and quantified. The three strains displayed similar growth patterns during the incubation (Fig. 3A). The levels of DSF and BDSF in the cultures of strain Δ*rpfB* increased slowly, probably due to the presence of the synthase RpfF. DSF and BDSF in the cultures of strains XC1 and Δ*rpfB*(*rpfB*) decreased progressively (Fig. 3B and C). After incubation for 2 h, the level of BDSF in the culture supernatant of XC1, Δ*rpfB* and Δ*rpfB*(*rpfB*) was 4.9 μM, 8.7 μM and 0 μM respectively. The level of DSF in the culture supernatant of the three strains was 9.6 μM, 15.5 μM and 1.45 μM respectively (Fig. 3B and C).

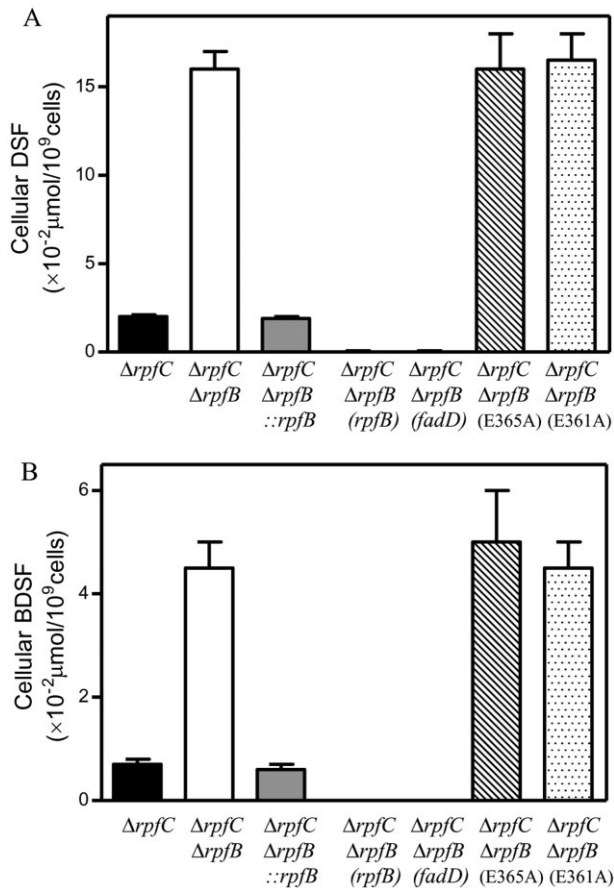**Fig. 2.** Cellular DSF and BDSF levels of *Xcc* strains. (A) DSF production and (B) BDSF production. Data are expressed as the means ± one standard deviation of three independent assays. Δ*rpfC*δ*rpfB*(E365A) indicates the *rpfB* and *rpfC* double mutant overexpressing RpfB with a point mutation at Glu[365] via the expression vector pLAFR3. Δ*rpfC*δ*rpfB*(E361A) indicates the *rpfB* and *rpfC* double mutant overexpressing FadD with a point mutation at Glu[361].

As a control, sodium oleate was also added into the cultures of three strains XC1, Δ*rpfB* and Δ*rpfB*(*rpfB*) to test the FCL activity of RpfB. The results showed that sodium oleate was rapidly utilized by all the three *Xcc* strains. After incubation for 60 min, the sodium oleate levels in the cultures of XC1, Δ*rpfB* and Δ*rpfB*(*rpfB*) were 5.5 μM, 11.5 μM and 0.4 μM respectively (Fig. 3D). These results were in agreement with previous findings that low-level expression of RpfB complements the growth of an *Escherichia coli fadD* strain on oleate (Bi *et al.*, 2014).

RpfB FCL enzymatic activity is required for DSF and BDSF turnover

FadD has been well studied as an FCL that plays a crucial role in fatty acid β-oxidation in *E. coli*. Two residues (T-214 and E-361) were identified to be essential for its catalytic activity (Weimar *et al.*, 2002). In the present study, *fadD*

was expressed in *Xcc* strains Δ*rpfB* and Δ*rpfC*Δ*rpfB*, and the levels of cellular DSF and BDSF, or those in the culture supernatants, were determined. Our results showed that *fadD* functionally complemented the strains Δ*rpfB* and Δ*rpfC*Δ*rpfB* for DSF and BDSF turnover
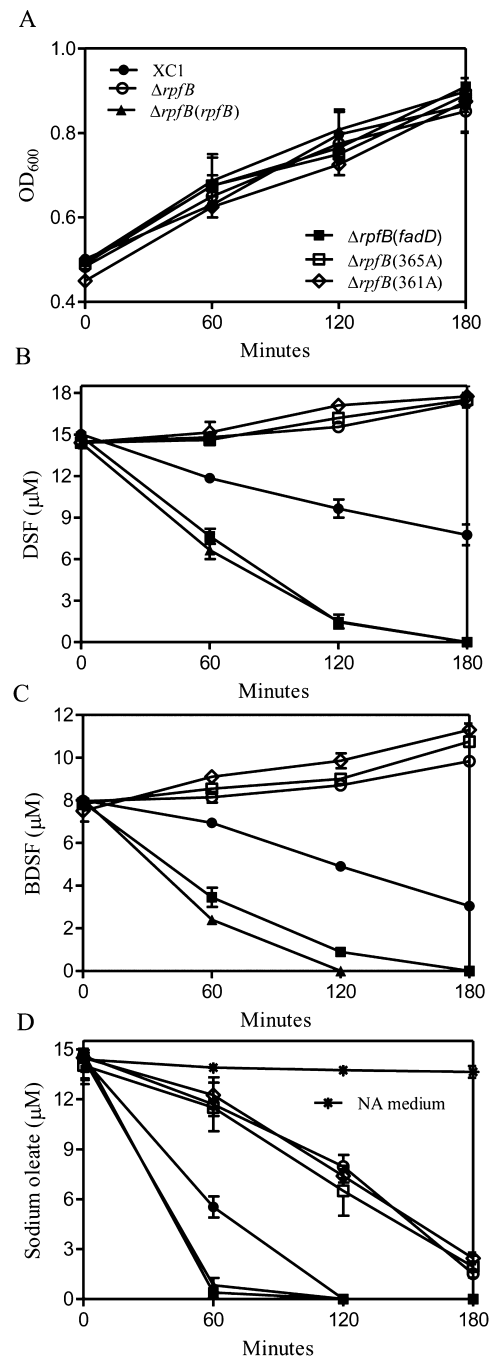

Fig. 3. DSF, BDSF and sodium oleate levels in the cultures of *Xcc* strains. (A) Growth time-course of *Xcc* cultures, (B) DSF, (C) BDSF and (D) sodium oleate. Data are expressed as the means ± one standard deviation of three independent assays.
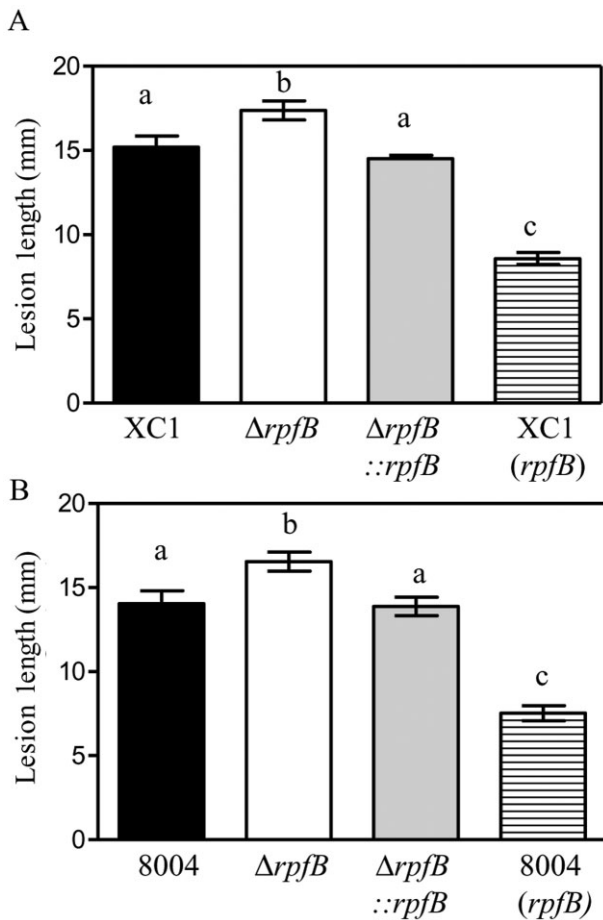
A

B

Fig. 4. Virulence of *Xcc* strains on Chinese radish. (A) Lesion length of *Xcc* wild-type strain XC1 and the derived strains. (B) Lesion length of *Xcc* wild-type strain 8004 and the derived strains. Virulence of the *Xcc* strains was tested by measuring lesion length after introducing bacteria into the vascular system of Chinese radish 'Manjianghong' by leaf clipping. Values are expressed as the mean and standard deviation of triplicate measurements, each comprising 20 leaves. Different letters indicate significant differences between treatments (LSD at $P = 0.05$).

(Figs 1–3A and B). Point mutation of the residue E-361 in FadD abolished its signal turnover activity (Figs 1–3A and B).

Bi and colleagues (2014) showed that RpfB functionally complemented the *E. coli* Δ*fadD* strain for growth on fatty acids as the sole carbon source, and the key residue E-365 was critical for the catalytic activity of RpfB FCL. The present study further showed that the point mutation in E-365 of RpfB abolished the activity of DSF and BDSF turnover (Figs 1–3A and B). Point mutation of the key residue glutamine in both FadD and RpfB significantly decreased the sodium oleate-utilizing activity (Fig. 3D). RpfB was expressed in *E. coli* and purified by affinity chromatography (Fig. S6A). The polyclonal antibody against RpfB was generated (Fig. S6B). Immunoblotting

analysis revealed that the mutation of E-365 to A-365 did not affect RpfB expression (Fig. S6C).

rpfB is involved in Xcc virulence

In the present study, *rpfB*-related phenotypes were examined by using the strains Δ*rpfB*, Δ*rpfB::rpfB* and *Xcc* (*rpfB*) that were derived from two *Xcc* wild-type strains, XC1 and 8004. Deletion of *rpfB* in *Xcc* strain 8004 had little effect on bacterial growth (Bi *et al.*, 2014). All the XC1-derived strains displayed similar growth patterns in the NA medium (Fig. 1A). In both *Xcc* strains, deletion of *rpfB* slightly enhanced the activities of the extracellular protease, amylase and cellulase by 9–21% respectively (Table S1). However, the observed increase was not statistically significant. *In trans* overexpression of *rpfB* in two wild-type *Xcc* strains resulted in a significant decrease in the production of extracellular enzymes by 30–46% in XC1 and by 35–38% in 8004 (Table S1).

Deletion of *rpfB* resulted in a significant increase in extracellular polysaccharide (EPS) production by about 25% in strain XC1 and by 30% in strain 8004 (Table S2). Overexpression of *rpfB* led to a significant decrease in EPS production by 44% in strain XC1 and by 40% in strain 8004 (Table S2).

To further evaluate whether RpfB contributes to *Xcc* virulence, a leaf clipping virulence assay using Chinese radish was conducted. The lesion length of wild-type strains XC1 and 8004 on Chinese radish was 15.2 mm and 14.0 mm, respectively, 2 weeks after inoculation (Fig. 4). Deletion of *rpfB* resulted in a significantly increased lesion length (17.3 mm and 16.5 mm, respectively), whereas overexpression of *rpfB* led to significantly reduced lesion length (8.5 mm and 7.5 mm, respectively) (Fig. 4). The lesion length of strains Δ*rpfB::rpfB* was not significantly different from that of the wild-type strains (Fig. 4).

RpfB expression is growth phase-dependent

The expression of *rpfB* in wild-type XC1 was first examined by using real-time quantitative reverse-transcriptase polymerase chain reaction (qRT-PCR) analysis. A two-fold increase in the transcriptional level of *rpfB* was observed at the late exponential stage (24 h) in NA liquid medium compared with that observed at mid-exponential stage (12 h) (Fig. 5A). At the early stationary growth stage (36 h), the expression level of *rpfB* was slightly reduced, but still higher than that observed at the mid-exponential stage (12 h) (Fig. 5A). The protein level of RpfB in wild-type *Xcc* was further examined using immunoblotting analysis. The RpfB level was low in the mid-exponential stage (12 h), and then slightly increased at the late exponential stage (24 h). The maximum RpfB level was
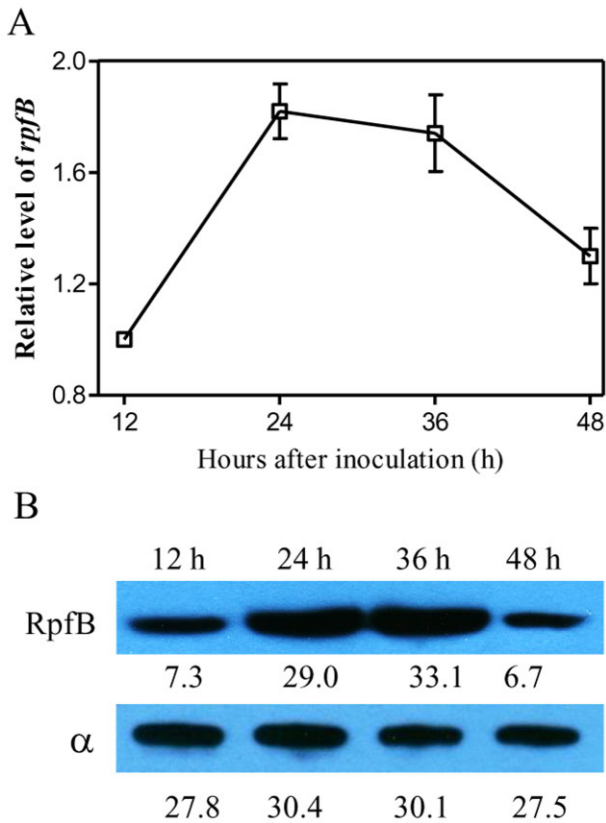
A

enous addition of DSF at a final concentration of 1.0 μM reduced RpfB expression to that of the wild-type level (Fig. 6B). However, exogenous addition of DSF at a final concentration of 10.0 μM to *rpfF* mutant strain Δ*rpfF*
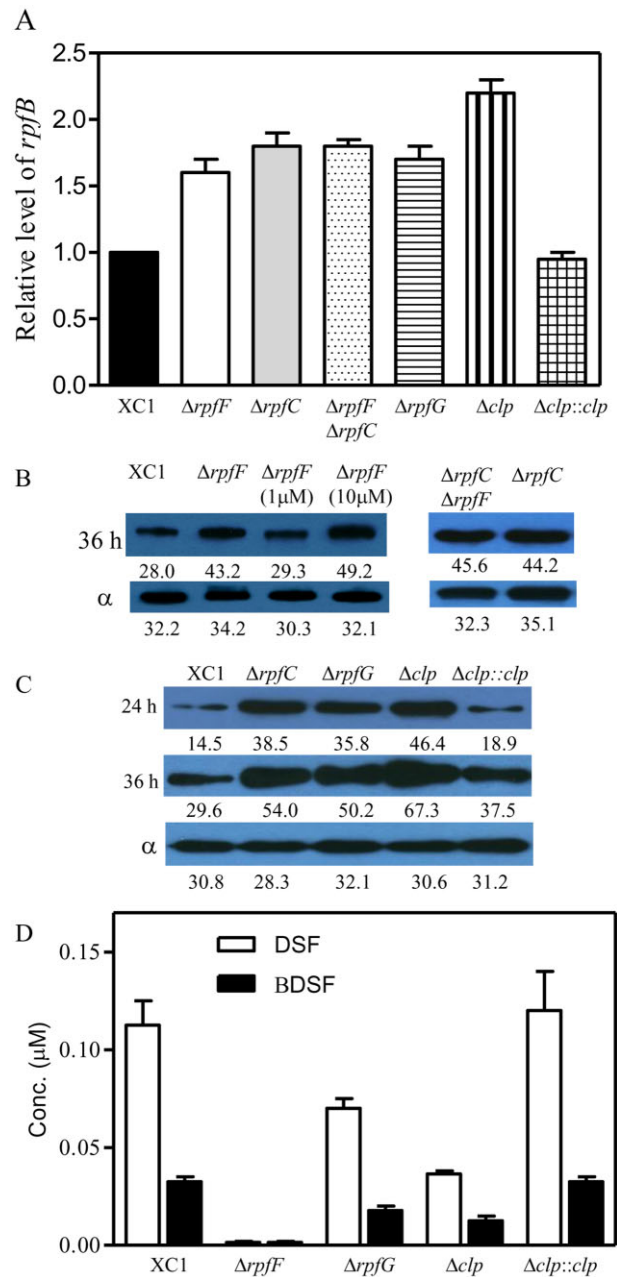
A

B

C

D

Fig. 5. *rpfB* expression in *Xcc* strain XC1 during growth in NA liquid medium. (A) Relative *rpfB* level as determined by real-time quantitative RT-PCR. (B) Relative RpfB level as determined by immunoblotting. (*Upper*) Western blot probed with an antibody against RpfB; (*lower*) Western blot probed with an antibody against the α subunit of RNA polymerase, which was used as a control for sample loading. The numbers indicate signal intensity as measured by using the IMAGEJ software (http://rsb.info.nih.gov/ij/).

observed at the early stationary stage (36 h) (Fig. 5B). At the late stationary stage (48 h), RpfB level was reduced, but still higher than that observed at the mid-exponential stage (Fig. 5B).

RpfB expression is differentially regulated by DSF signal in a concentration-dependent manner

RpfF is a key enzyme required for DSF biosynthesis. In the present study, the expression of *rpfB* at both transcriptional and translational levels at 24 h–36 h after inoculation in *rpfF* deletion strain Δ*rpfF* was examined. The qRT-PCR analysis showed that mutation of *rpfF* led to a significant increase in the expression of *rpfB* at the transcriptional level (Fig. 6A). Exogenous addition of DSF (0.5–2.5 μM) restored *rpfB* expression to that of the wild-type level, whereas addition of DSF (10.0–50.0 μM) significantly increased *rpfB* expression (data not shown). Western blotting analysis showed that a mutation in *rpfF* resulted in an increase in RpfB expression, and exog-

Fig. 6. The expression of RpfB in *Xcc* strains. (A) Relative *rpfB* level in the strains XC1, Δ*rpfF*, Δ*rpfC*, Δ*rpfG*, Δ*clp*, Δ*clp*::*clp* as determined by real-time quantitative RT-PCR. (B) Protein levels of RpfB in the strains XC1, Δ*rpfF*, Δ*rpfF*(1 μm) (the strain Δ*rpfF* supplemented with 1.0 μm DSF), Δ*rpfF*(10 μm) (the strain Δ*rpfF* supplemented with 10.0 μm DSF), and Δ*rpfC*Δ*rpfF*. (C) Protein levels of rpfb in the strains XC1, Δ*rpfC*, Δ*rpfG*, Δ*clp* and Δ*clp*:*clp*. (D) DSF and BDSF production in the *Xcc* strains XC1, Δ*rpfF*, Δ*rpfG*, Δ*clp* and Δ*clp*:*clp*. Δ*clp*:*clp* indicates *clp* deletion strains complemented by a single copy of *clp* in the *att*Tn7 site. The numbers indicate the signal intensities of RpfB as measured by using the IMAGEJ software.

significantly increased RpfB expression (Fig. 6B). No significant differences in *rpfB* expression were observed between DSF-overproducing strain ∆*rpfC* and DSF-deficient strain ∆*rpfC*∆*rpfF* (Fig. 6B), suggesting that the DSF-family signals do not directly regulate RpfB expression.

RpfB expression is negatively regulated by DSF signalling cascade

DSF signalling involves the two-component system RpfC/RpfG, the second messenger c-di-GMP and the global regulator Clp in *Xcc* (He and Zhang, 2008; Deng *et al.*, 2011). S1 nuclease protection assay revealed that *rpfB* expression was upregulated by RpfC (Slater *et al.*, 2000). These findings suggest that *rpfB* expression might be controlled by the DSF signalling pathway. To test this hypothesis, the expression of *rpfB* at both transcriptional and translational levels at 24 h after inoculation in a set of *rpf* deletion mutants and *clp* deletion strain ∆*clp* was examined. The qRT-PCR analysis showed that mutation of *rpfC*, *rpfG* or *clp* led to an increase in expression of *rpfB* at the transcriptional level, among which strain ∆*clp* showed the highest expression level (Fig. 6A). Mutation in *rpfC*, *rpfG* or *clp* also resulted in the upregulation of RpfB; complementation with a single copy of *clp* in the strain ∆*clp* restored RpfB expression to that of the wild-type level (Fig. 6C). These findings suggest that the DSF signal transduction cascade represses RpfB expression.

To further support the above conclusion, DSF and BDSF production in strains XC1, ∆*rpfF*, ∆*rpfG* and ∆*clp* were compared at 36 h after inoculation. As expected, no DSF and BDSF production was detected in the strain ∆*rpfF* (Fig. 6D), and about 38–60-fold increase in DSF and BDSF production was observed in the strain ∆*rpfC* (Fig. S2). The DSF production in strains ∆*rpfG* and ∆*clp* decreased by 38% and 60% respectively (Fig. 6D). The BDSF production in these two strains decreased by 45% and 61% respectively (Fig. 6D). The decreased production in both DSF and BDSF levels in the *rpfG* mutant is in agreement with previous bioassay results that deletion of *rpfG* results in less DSF production in the *Xoo* strain KACC 10331 (He *et al.*, 2010).

In the *Xcc* genome, *rpfF* is located downstream of *rpfB*. S1 nuclease protection assay showed that *rpfF* and *rpfB* are within separate transcriptional units, although there is evidence that some readthrough occurs from *rpfB* to *rpfF* (Slater *et al.*, 2000). RpfB was shown to be absolutely not required for DSF synthesis in *X. fastidiosa*, and mutations in *Xcc*-disrupting *rpfB* apparently have a polar effect on the downstream *rpfF* (Almeida *et al.*, 2012). In the present study, to further investigate whether the deletion of *rpfC*, *rpfG* or *clp* affects *rpfF* expression, RpfF levels in these strains were analysed using a polyclonal antibody against

RpfF (Fig. S7A). The results showed that deletion of *rpfC* results in overexpression of RpfF (Fig. S7B), whereas the deletion of *rpfG* or *clp* had little effect on RpfF expression (Fig. S7C). Therefore, DSF and BDSF overproduction in the *rpfC* mutant is the final result of a significant increase in DSF biosynthesis and a slight increase in DSF turnover. The observed DSF and BDSF reduction in the strains ∆*rpfG* and ∆*clp* was mainly due to the increase in signal turnover.

Clp directly binds to the promoter of rpfB *to repress its expression*

Clp is a conserved global transcriptional regulator that is essential for DSF-dependent regulation of virulence factor production (He *et al.*, 2007; Chin *et al.*, 2010; Tao *et al.*, 2010). Deleting *clp* resulted in the upregulation of *rpfB* (Fig. 6), which suggests that Clp might have been directly binding to the promoter region of *rpfB* to regulate its transcription. To test this hypothesis, the putative promoter DNA fragment covering 431 bp upstream of the *rpfB* translational start site, namely P$_{rpfB}$, was cloned and labelled for analysis using electrophoretic mobility shift assays (EMSA). The addition of purified Clp protein, ranging from 0.35 µg to 1.4 µg, to the reaction mixtures (20 µl and at 25°C) caused a shift in the mobility of the labelled P$_{rpfB}$ DNA fragment, which is suggestive of the formation of a Clp-P$_{rpfB}$ complex (Fig. 7A and B). The addition of unlabelled P$_{rpfB}$ to the reaction mixture significantly reduced the formation of the labelled Clp-P$_{rpfB}$ complex. The second messenger cyclic-di-GMP has been shown to interfere with Clp binding to its cognate promoter in *Xcc* (Chin *et al.*, 2010; Tao *et al.*, 2010). In the present study, c-di-GMP at different concentrations was added to the reaction mixture containing a saturating amount of Clp (1.4 µg). Our results showed that c-di-GMP at 10 µM and 20 µM partially prevented the formation of the Clp-P$_{rpfB}$ complex; c-di-GMP at 40 µM completely blocked the binding between Clp and P$_{rpfB}$ (Fig. 7B).

To further identify the Clp binding site in the promoter P$_{rpfB}$, DN*ase* I footprinting analysis was conducted. The results revealed that Clp protects a region from −30 to −66 bp relative to the transcription start site of *rpfB* (Fig. 7C). This region comprises two subregions, namely I (from −30 to −46) and II (from −48 to −66) as nucleotide A (at the antisense strand) at −47 position was determined to be hypersensitive to DNase I, indicating an alteration in the secondary structure induced by Clp binding to P$_{rpfB}$ (Fig. 7C). An imperfect palindromic AATGC-tgctgc-GCATC motif was identified as the putative Clp binding site on P$_{rpfB}$ (Fig. 7C). Point mutation of TGC of the putative binding motif to AAA abolished Clp binding to P$_{rpfB}$ in the EMSA assay (Fig. 7D). Further point mutation of TGC to AAA in the promoter region of *rpfB* was conducted in
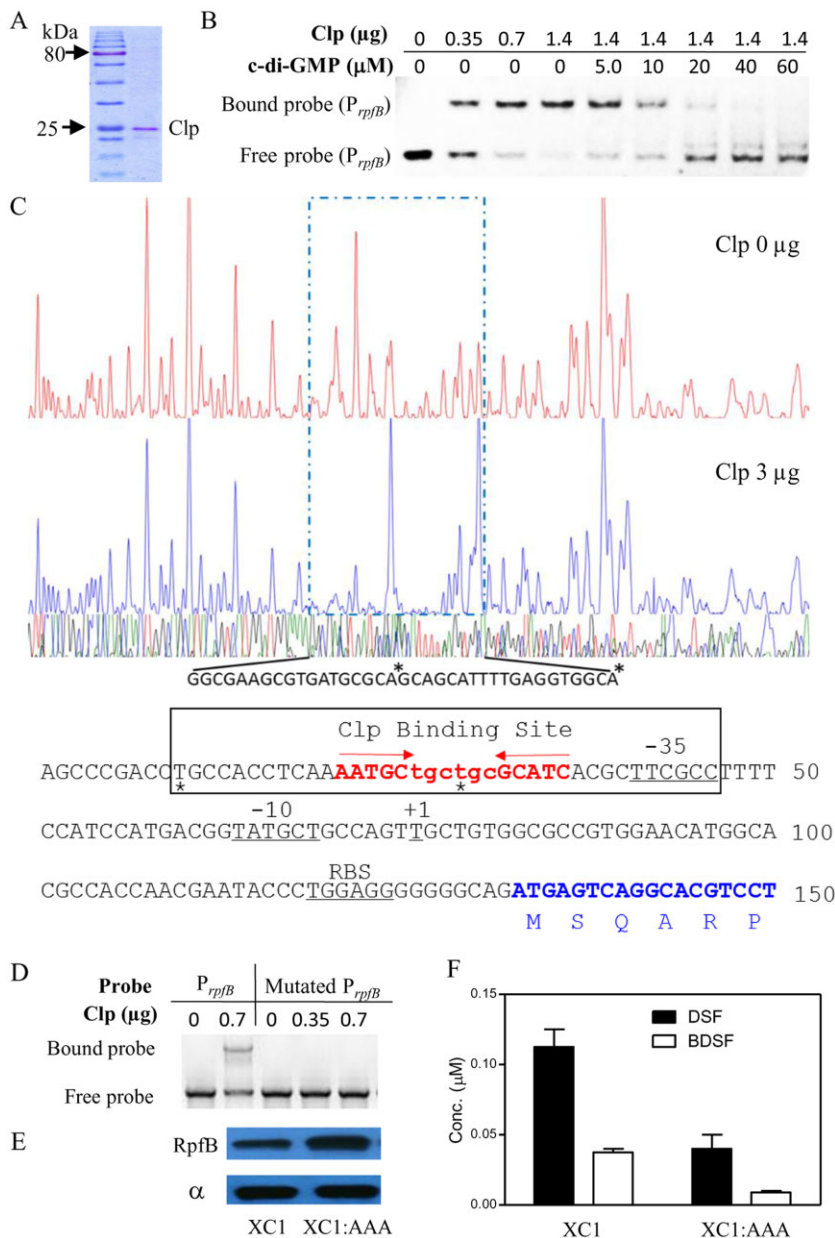
Fig. 7. Identification of Clp binding site at the promoter region of *rpfB* (p*rpfB*).
A. SDS-PAGE analysis of purified Clp protein.
B. Formation of Clp-p*rpfB* complex as assayed by EMSA, and competition binding was induced by adding cyclic-di-GMP.
C. DN*ase* I footprinting assay of Clp binding to p*rpfB*. Approximately 700 ng of the probe p*rpfB* that covers 431 bp upstream of the translational start codon of *rpfB* was incubated with 3 μg of Clp in the EMSA buffer. P*rpfB* was labelled with FAM dye and incubated with Clp (blue line in the middle) or without Clp (red line at the top). The region protected by Clp from DN*ase* I cleavage is indicated by a blue dotted box. The nucleotide sequence of the Clp protected region is shown at the bottom, in which the nucleotides hypersensitive to DN*ase* I are indicated by asterisks. The region protected by Clp is marked with a rectangle. The Clp binding site in p*rpfB* is shown in red bold letters, in which the imperfect palindrome sequence of the Clp binding site is indicated by arrows above the nucleotides. The transcription initiation site, −10/−35 sequences and ribosome-binding site (RBS) are underlined and labelled with +1, −10, −35 and RBS respectively. The initial 18 coding nucleotides of *rpfB* and the translated amino acids are shown in blue bold letters.
D. No complex formed between the mutated p*rpfB* and Clp.
E. RpfB level increased in the strain XC1::AAA, which harbours three point mutations (TGC→AAA) in the putative Clp binding site of the *rpfB* promoter.
F. DSF and BDSF production in the wild-type strain XC1 and the mutated strain XC1:AAA at 24 h after inoculation. Values are expressed as the mean and standard deviation of three independent measurements.

the XC1 chromosome, and the resulting strain XC1::AAA exhibited an upregulation of RpfB expression and a downregulation of DSF and BDSF production (Fig. 7E and F).

RpfB-dependent signal turnover system is present in a wide range of bacterial species

In the present study, by BLASTing the Nr database in National Center for Biotechnology Information (NCBI), we found that RpfB, the *rpf* cluster and Clp were not only present in the genomes of all *Xanthomonas* species, but also present in *X. fastidiosa* (*Xyl*), *Stenotrophomonas maltophilia* (*Stm*), *Lysobacter dokdonensis DS-58*

(*Lys*), *Pseudoxanthomonas spadix* BDA-59 (*Psx*), *Methylobacillus flagellatus* (*Mfl*) and *Thiobacillus denitrificans* (*Tbd*) (Fig. S8A). The putative Clp binding site was also found in the promoter regions of *rpfB* homologous in other *Xanthomonas* species such as *Xoo*, *Xanthomonas axonopodis* pv. *citri* (*Xac*), *Xanthomonas fuscans* subsp. *fuscans* (*Xff*) and *Xanthomonas hortorum* pv. *carotae* (*Xhc*) (Fig. S8B). These findings suggest that RpfB-dependent signal turnover is a conserved mechanism in bacteria.

Discussion

In *Xcc*, DSF accumulates during the early stationary phase and its level subsequently declines sharply (Barber

et al., 1997; Wang *et al.*, 2004), which is indicative of the presence of a naturally occurring DSF signal turnover system. Recent studies have shown that RpfB possesses FCL activity and activates a wide range of fatty acids to their CoA esters *in vitro* (Bi *et al.*, 2014). The present study demonstrated that RpfB expression is cell density-dependent and was significantly enhanced when *Xcc* cell growth enters the stationary phase. RpfB effectively turns over DSF and BDSF signals *in vivo* (Figs 1–3). Therefore, RpfB represents a naturally occurring signal turnover system that targets DSF-family QS signals in *Xcc*. This system is not only present in all *Xanthomonas* species, but also present in a wide range of non-*Xanthomonas* species (Fig. S8B), suggesting that it is a conserved mechanism in bacteria.

FadD is a well-studied FCL in *E. coli* (Weimar *et al.*, 2002). FadD and RpfB had similar effects on DSF and BDSF turnover in *Xcc* (Figs 1–3). Both enzymes share the key catalytic residue glutamine (E-361 in *E. coli*, E-365 in *Xcc*) that is required for FCL activity (Bi *et al.*, 2014). The present study further demonstrated that the key glutamine residue is essential for RpfB- or FadD-dependent signal turnover (Figs 1–3). Therefore, it seems that RpfB uses FCL activity to convert DSF and BDSF signals in *Xcc*. However, it would be of interest to determine why RpfB displays FCL activity towards DSF and BDSF within the cell, but not in the *in vitro* reaction mixture. At least two potential mechanisms may address this discrepancy. One is that RpfB-dependent DSF and BDSF turnover requires additional factors such as co-factors, metals or salts, which is only present in *Xcc*, but not in the reaction mixture. Another possibility is that RpfB adopts different conformations in *in vivo* and *in vitro* conditions. Further clarification of these possible mechanisms will help elucidate the mechanism of RpfB-dependent DSF-family signal turnover.

The first naturally occurring QS signal turnover system was reported in *A. tumefaciens*, which consists of at least an AHL degradation enzyme BlcC (formerly AttM) and a negative transcription factor BlcR (formerly AttJ) (Zhang *et al.*, 2002). The expression of *blcC* is tightly controlled by the transcriptional repressor BlcR. Carbon and nitrogen source starvation, γ-butyrolactone, γ-hydroxybutyrate, and succinic semialdehyde can all release the repression exerted by BlcR, hence allowing the expression of the *blcC* gene (Lang and Faure, 2014). The mechanism of naturally occurring DSF signals turnover in *Xcc* is similar to that observed in *A. tumefaciens*, which consists of at least RpfB and the transcriptional regulator Clp. The expression of *rpfB* is partially repressed by the regulator Clp, and the second messenger c-di-GMP can release the repression exerted by Clp (Fig. 7B). The present study suggests that a high level of DSF-family signals triggers c-di-GMP degradation via the two-component system, RpfC/RpfG, thus

possibly facilitating in the expression of *rpfB*. The *Xcc* genome encodes multiple proteins involved in c-di-GMP biosynthesis and degradation. Previous findings have demonstrated that *Xcc* integrates information from diverse environmental inputs to modulate virulence factor synthesis via c-di-GMP signalling systems (Ryan *et al.*, 2007; He *et al.*, 2009). Therefore, the expression of *rpfB* might also be controlled by other environmental factors.

Clp has been well studied as a cyclic di-GMP-responsive transcriptional regulator that plays essential roles in virulence factor production and the DSF signalling network in *Xcc* (He *et al.*, 2007; Chin *et al.*, 2010; Tao *et al.*, 2010). In most cases, Clp acts a transcriptional activator in *Xcc* (He *et al.*, 2007; Liu *et al.*, 2013). The present study demonstrated that Clp acts as a repressor in the regulation of *rpfB* expression (Fig. 7). This is consistent with the result in another study that Clp can act as both an activator and repressor of transcription of different genes (*rsmA* and *xag*) to influence biofilm formation as a response to cyclic di-GMP (Lu *et al.*, 2012). In addition, Clp has been shown to recognize the conserved DNA-binding site (TGTGA-N6-TCACA) (He *et al.*, 2007; Chin *et al.*, 2010). The present study identified an imperfect palindromic AATGC-N6-GCATC motif as the putative Clp binding site in *rpfB* promoter in *Xcc* (Fig. 7). The same binding site was also found in the promoter regions of *rpfB* homologues in other *Xanthomonas* species (Fig. S8B). This newly identified Clp binding site shares only 2/5 of the highly conserved residues in each of the right and left arms of the previously identified Clp-binding motif. Whether this limited conservation is associated with Clp's role as a repressor of *rpfB* transcription remains to be elucidated.

The pattern of fatty acid utilization as the sole carbon source in *Xcc* is very similar to that observed in *E. coli* (Campbell *et al.*, 2003). In *E. coli*, expression of the *fad* genes of the fatty acid degradation regulon is regulated by the repressor, FadR, the oxygen-sensitive ArcA-ArcB two-component system, and the cyclic AMP (cAMP) receptor protein-cyclic AMP (CRP-cAMP) complex (Feng and Cronan, 2012). *Xcc* contains several putative homologues for fatty acid metabolism, including RpfB, FadA (Xcc1978), FadB (Xcc1979, Xcc0810), FadJ (Xcc1266), FadE (Xcc1261), and FadH (Xcc0933) and CRP homologue Clp, but lacks an FadR homologue. Bi and colleagues (2014) clearly demonstrated the roles of RpfB in fatty acid and lipid metabolism in *Xcc*. The present study further showed that RpfB is responsible for DSF-family signal turnover. Based on these findings, we propose that RpfB might have different functions at various growth stages. At the early stages of growth, *Xcc* cells produce a basal level of DSF-family signals, and RpfB expression is partially repressed by Clp. A low level of RpfB mainly activates the free fatty acids, yielding acyl-CoAs for membrane lipid synthesis. During growth,

DSF-family signals accumulate. When bacterial cell growth enters the stationary phase to reach a sufficiently high population density, the accumulated DSF-family signals interact with the sensor protein, RpfC, to trigger the expression of DSF-dependent genes via the signalling cascade involving RpfG, c-di-GMP and Clp. At the same time, RpfB expression is also enhanced by the same DSF signalling cascade and functions in signal turnover as well as activation of other fatty acids. In consequence, the level of DSF-family signals declines and *Xcc* cells exit the QS phase, and RpfB expression returns to a low level to facilitate activation of free fatty acids. The evolution of such fine-tuned genetic system for *rpfB* expression and the multiple roles of RpfB ensure precise and economically controlled QS-dependent traits and basic fatty acid metabolism in *Xcc*.

Experimental procedures

Bacterial strains, plasmids and culture conditions

The bacterial strains and plasmids used in the present study are listed in Table S3. In most experiments, *Xcc* strains were grown at 30°C in NA medium (5 g l^{-1} peptone, 3 g l^{-1} beef extract, 10 g l^{-1} sucrose, 1 g l^{-1} yeast extract, pH 7.0) or NYG medium (5 g l^{-1} peptone, 3 g l^{-1} yeast extract, 20 g l^{-1} glycerol, pH 7.0). *Escherichia coli* strains were grown at 37°C in Luria Bertani (LB) medium (10 g l^{-1} tryptone, 5 g l^{-1} yeast extract, 10 g l^{-1} NaCl, pH 7.0). For culture medium preparation, tryptone, peptone, beef extract and yeast extract were purchased from Sangon Biotech (Shanghai, China). Where required, antibiotics were used at a concentration of 25 μg·ml^{-1} for rifampicin and kanamycin, 20 μg ml^{-1} for gentamicin, 10 μg ml^{-1} for tetracycline, and 100 μg ml^{-1} for ampicillin. Bacterial growth was determined by measuring optical density at a wavelength of 600 nm.

Construction of in frame deletion mutants and complementation

The *Xcc* wild-type strains XC1 and 8004 were used as parental strains for the generation of deletion mutants, as previously described (He *et al.*, 2006b). The primers used are listed in Table S4. For single-copy complementation of *rpfB*, the coding region of *rpfB* plus 431 bp upstream of the translational start codon of *rpfB* was PCR-amplified and cloned into a versatile Mini-Tn7 delivery vector mini-Tn7T-Gm. The resulting constructs were transferred into *Xcc* by electroporation, following methods described elsewhere (Jittawuttipoka *et al.*, 2009). For RpfB overexpression, its coding region was PCR-amplified and cloned into the MCS site of the expression cosmid, pLAFR3. The resulting construct was transferred into *Xcc* by triparental mating.

Extraction, purification and quantitative analysis of BDSF and DSF using LC-MS

The extraction of DSF and BDSF in *Xcc* culture supernatants was conducted following the methods previously described (He *et al.*, 2010). To quantify DSF and BDSF production in the culture of strain Δ*rpfC*, 0.2 ml of the supernatant was collected. Its crude ethyl acetate extract was passed through a 0.45 μm Minisart filter unit and was then condensed to 0.1 ml for LC-MS analysis. To quantify DSF and BDSF production in the culture of the wild-type strain XC1, 20.0 ml of the supernatant was collected. To determine the levels of cellular DSF and BDSF, cell pellets were collected from 100 ml of Δ*rpfC* cultures at 36 h after inoculation, and washed for twice using 1 × PBS buffer. The resulting cell pellets were dissolved in 5 ml of B-PER® Bacterial Protein Extraction Reagent (Prod# 90084) with lysozyme (100 μg ml^{-1}) and DNase I (150 U ml^{-1}) at room temperature for 5 min. The extracts were then heated at 95°C for 5 min to denature the total protein. After centrifugation at 12 000 r.p.m. (Thermo) for 10 min at 4°C, the supernatants were collected for DSF extraction as previously described (He *et al.*, 2010).

The crude ethyl acetate crude extracts were then condensed to a volume of 0.1 ml for LC-MS analysis. Three microlitres of the condensed samples were applied to an ultra performance liquid chromatographic system (Agilent 1290 Infinity) on a Zorbax XDB C18 reverse phase column (4.6 × 150 mm, temperature-controlled at 30°C), and eluted with methanol-water (80:20, v/v) at a flow rate of 0.4 ml min^{-1} in a diode array detector (Agilent G4212A). Data were acquired in the centroid mode using the Agilent MassHunter Workstation Data Acquisition Software (revision B.04). The BDSF and DSF levels in the culture supernatant were quantified using peak intensity (PI) in the extracted ion chromatogram according to the following formula: BDSF (μM) = $9.60 \times 10^{-7} \times$ PI −0.53, DSF (μM) = $9.83 \times 10^{-7} \times$ PI −0.20. The formula was derived from a dose–PI plot in the LC-MS chromatogram using various dilutions of synthetic BDSF and DSF signals, with a correlation coefficient (R^2) of 0.998 and 0.996 respectively.

Quantitative determination of extracellular enzyme activity and EPS production and virulence testing

The method for quantitative determination of extracellular enzyme activity and EPS production was previously described (He *et al.*, 2006b). The virulence of *Xcc* to Chinese radish was estimated by leaf clipping as earlier described (Ryan *et al.*, 2007). Twenty leaves from each tested strain were inoculated. Lesion length was measured 2 weeks after inoculation. Each strain was tested in at least three separate experiments.

Total RNA extraction and RT-PCR for transcription analysis

Total RNA was isolated using the RNeasy Miniprep Kit (Qiagen). The PrimeScript® RT reagent kit was used for real-time quantitative RT-PCRs. Quantification of gene expression and melting curve analysis were performed using Mastercycler ep Realplex 4S (Eppendorf) and SYBR® Premix Ex Taq (Takara). The constitutively expressed 16S rRNA gene was used as reference to standardize all samples and replicates.

Protein expression and purification

The RpfB protein was expressed and purified following the procedure previously described (Bi *et al.*, 2014). Clp and RpfF proteins were expressed and purified as described elsewhere (He *et al.*, 2006a; Tao *et al.*, 2010). The protein samples were stored as aliquots in 20% (vol/vol) glycerol at −20°C until analysis.

Western blot analysis

Western blot analysis was performed as described elsewhere (Green and Sambrook, 2012). The RpfB and RpfF proteins were used as antigen to obtain polyclonal antisera by immunizing rabbits through subcutaneous injections at 2-week intervals. The hybridization signal was detected using the SuperSignal West Pico Chemiluminescent Substrate (PIERCE, USA). The monoclonal antibody against the α subunit of RNA polymerase (NeoClone) was used as a control for sample loading. Analysis of variance for experimental datasets was performed using the IMAGEJ software (version 1.48).

EMSA and DNase I footprinting assay

The promoter region of *rpfB* covering 431 bp upstream of the *rpfB* translational start codon, P$_{rpfB}$, was cloned into the T-vector of pTA2 (TOYOBO) as template. Fluorescent FAM-labelled P$_{rpfB}$ probes were PCR-amplified using the primers listed in Table S4. Electrophoretic mobility shift assay was performed using the LightShift Chemiluminescent EMSA Kit (Thermo Scientific Pierce) in a 20 μl reaction mixture at 25°C. Cyclic-di-GMP was purchased from Invitrogen. Sheared salmon sperm DNA (100 ng μl^{-1}) was added to prevent non-specific binding. DNase I footprinting assays were performed as previously described (Wang *et al.*, 2012).

Site-directed mutagenesis

fadD, *rpfB* and its promoter region, PrpfB, were respectively cloned into pTA2 for point mutation analysis using QuickChange Site-Directed Mutagenesis Kit (Agilent Technologies). The primers used are listed in Table S4. The mutated *fadD* or *rpfB* was cloned to the expression vector, pLAFR3, and the resulting construct was further transferred into the *Xcc* strains by triparental mating. The mutated PrpfB was further cloned into the suicide vector, pK18mobsacB. The recombinant construct was mobilized into *Xcc*. The strains with point mutations in PrpfB in the XC1 chromosome were further verified by PCR amplification, followed by DNA sequencing.

Acknowledgements

References

Almeida, R.P., Killiny, N., Newman, K.L., Chatterjee, S., Ionescu, M., and Lindow, S.E. (2012) Contribution of *rpfB* to cell-to-cell signal synthesis, virulence, and vector transmission of *Xylella fastidiosa*. *Mol Plant Microbe Interact* **25:** 453–462.

Barber, C.E., Tang, J.L., Feng, J.X., Pan, M.Q., Wilson, T.J., Slater, H., *et al.* (1997) A novel regulatory system required for pathogenicity of *Xanthomonas campestris* is mediated by a small diffusible signal molecule. *Mol Microbiol* **24:** 555–566.

Bi, H., Christensen, Q.H., Feng, Y., Wang, H., and Cronan, J.E. (2012) The *Burkholderia cenocepacia* BDSF quorum sensing fatty acid is synthesized by a bifunctional crotonase homologue having both dehydratase and thioesterase activities. *Mol Microbiol* **83:** 840–855.

Bi, H., Yu, Y., Dong, H., Wang, H., and Cronan, J.E. (2014) *Xanthomonas campestris* RpfB is a fatty Acyl-CoA ligase required to counteract the thioesterase activity of the RpfF diffusible signal factor (DSF) synthase. *Mol Microbiol* **93:** 262–275.

Campbell, J.W., Morgan-Kiss, R.M., and Cronan, J.E., Jr (2003) A new *Escherichia coli* metabolic competency: growth on fatty acids by a novel anaerobic beta-oxidation pathway. *Mol Microbiol* **47:** 793–805.

Chin, K.H., Lee, Y.C., Tu, Z.L., Chen, C.H., Tseng, Y.H., Yang, J.M., *et al.* (2010) The cAMP receptor-like protein CLP is a novel c-di-GMP receptor linking cell-cell signaling to virulence gene expression in *Xanthomonas campestris*. *J Mol Biol* **396:** 646–662.

Deng, Y., Wu, J., Tao, F., and Zhang, L.H. (2011) Listening to a new language: DSF-based quorum sensing in Gram-negative bacteria. *Chem Rev* **111:** 160–173.

Dong, Y.H., Wang, L.Y., and Zhang, L.H. (2007) Quorum-quenching microbial infections: mechanisms and implications. *Philos Trans R Soc Lond B Biol Sci* **362:** 1201–1211.

Draganov, D.I., Teiber, J.F., Speelman, A., Osawa, Y., Sunahara, R., and La Du, B.N. (2005) Human paraoxonases (PON1, PON2, and PON3) are lactonases with overlapping and distinct substrate specificities. *J Lipid Res* **46:** 1239–1247.

Feng, Y., and Cronan, J.E. (2012) Crosstalk of *Escherichia coli* FadR with global regulators in expression of fatty acid transport genes. *PLoS ONE* **7:** e46275.

Green, M.R., and Sambrook, J.R. (2012) *Molecular Cloning: A Laboratory Manual*, 4th edn. New York: Cold Spring Harbor Laboratory Press.

He, Y.W., and Zhang, L.H. (2008) Quorum sensing and virulence regulation in *Xanthomonas campestris*. *FEMS Microbiol Rev* **32:** 842–857.

He, Y.W., Wang, C., Zhou, L., Song, H., Dow, J.M., and Zhang, L.H. (2006a) Dual signaling functions of the hybrid sensor kinase RpfC of *Xanthomonas campestris* involve either phosphorelay or receiver domain-protein interaction. *J Biol Chem* **281:** 33414–33421.

He, Y.W., Xu, M., Lin, K., Ng, Y.J., Wen, C.M., Wang, L.H., *et al.* (2006b) Genome scale analysis of diffusible signal factor regulon in *Xanthomonas campestris* pv. *campestris*: identification of novel cell-cell communication-dependent genes and functions. *Mol Microbiol* **59:** 610–622.

He, Y.W., Ng, A.Y., Xu, M., Lin, K., Wang, L.H., Dong, Y.H., *et al.* (2007) *Xanthomonas campestris* cell-cell communication involves a putative nucleotide receptor protein Clp and a hierarchical signalling network. *Mol Microbiol* **64:** 281–292.

He, Y.W., Boon, C., Zhou, L., and Zhang, L.H. (2009) Co-regulation of *Xanthomonas campestris* virulence by quorum sensing and a novel two-component regulatory system RavS/RavR. *Mol Microbiol* **71:** 1464–1476.

He, Y.W., Wu, J., Cha, J.S., and Zhang, L.H. (2010) Rice bacterial blight pathogen *Xanthomonas oryzae* pv. *oryzae* produces multiple DSF-family signals in regulation of virulence factor production. *BMC Microbiol* **10:** 187–196.

Jittawuttipoka, T., Buranajitpakorn, S., Fuangthong, M., Schweizer, H.P., Vattanaviboon, P., and Mongkolsuk, S. (2009) Mini-Tn7 vectors as genetic tools for gene cloning at a single copy number in an industrially important and phytopathogenic bacteria, *Xanthomonas* spp. *FEMS Microbiol Lett* **298:** 111–117.

Lang, J., and Faure, D. (2014) Functions and regulation of quorum-sensing in *Agrobacterium tumefaciens. Front Plant Sci.* **5:** 14–27.

Liu, Y.F., Liao, C.T., Song, W.L., Hsu, P.C., Du, S.C., Lo, H.H., and Hsiao, Y.M. (2013) GsmR, a response regulator with an HD-related output domain in *Xanthomonas campestris*, is positively controlled by Clp and is involved in the expression of genes responsible for flagellum synthesis. *FEBS J* **280:** 199–213.

Lu, X.H., An, S.Q., Tang, D.J., McCarthy, Y., Tang, J.L., Dow, J.M., and Ryan, R.P. (2012) RsmA regulates biofilm formation in *Xanthomonas campestris* through a regulatory network involving cyclic di-GMP and the Clp transcription factor. *PLoS ONE* **7:** e52646.

Newman, K.L., Chatterjee, S., Ho, K.A., and Lindow, S.E. (2008) Virulence of plant pathogenic bacteria attenuated by degradation of fatty acid cell-to-cell signaling factors. *Mol Plant Microbe Interact* **21:** 326–334.

Rutherford, S.T., and Bassler, B.L. (2012) Bacterial quorum sensing: its role in virulence and possibilities for its control. *Cold Spring Harb Perspect Med.* **2:** pii: a012427.

Ryan, R.P., and Dow, J.M. (2011) Communication with a growing family: diffusible signal factor (DSF) signaling in bacteria. *Trends Microbiol* **19:** 145–152.

Ryan, R.P., Fouhy, Y., Lucey, J.F., Crossman, L.C., Spiro, S., He, Y.W., *et al.* (2006) Cell-cell signaling in *Xanthomonas campestris* involves an HD-GYP domain protein that functions in cyclic di-GMP turnover. *Proc Natl Acad Sci USA* **103:** 6712–6717.

Ryan, R.P., Fouhy, Y., Lucey, J.F., Jiang, B.L., He, Y.Q., Feng, J.X., *et al.* (2007) Cyclic di-GMP signaling in the virulence and environmental adaptation of *Xanthomonas campestris. Mol Microbiol* **63:** 429–442.

Ryan, R.P., McCarthy, Y., Andrade, M., Farah, C.S., Armitage, J.P., and Dow, J.M. (2010) Cell-cell signal-dependent dynamic interactions between HD-GYP and GGDEF domain proteins mediate virulence in *Xanthomonas campestris. Proc Natl Acad Sci USA* **107:** 5989–5994.

Ryan, R.P., McCarthy, Y., Kiely, P.A., O'Connor, R., Farah, C.S., Armitage, J.P., *et al.* (2012) Dynamic complex formation between HD-GYP, GGDEF and PilZ domain proteins regulates motility in *Xanthomonas campestris. Mol Microbiol* **86:** 557–567.

Sio, C.F., Otten, L.G., Cool, R.H., Diggle, S.P., Braun, P.G., Bos, R., *et al.* (2006) Quorum quenching by an N-acyl-homoserine lactone acylase from *Pseudomonas aeruginosa* PAO1. *Infect Immun* **74:** 1673–1682.

Slater, H., Alvarez-Morales, A., Barber, C.E., Daniels, M.J., and Dow, J.M. (2000) A two-component system involving an HD-GYP domain protein links cell-cell signaling to pathogenicity gene expression in *Xanthomonas campestris. Mol Microbiol* **38:** 986–1003.

Tao, F., He, Y.W., Wu, D.H., Swarup, S., and Zhang, L.H. (2010) The cyclic nucleotide monophosphate domain of *Xanthomonas campestris* global regulator Clp defines a new class of cyclic di-GMP effectors. *J Bacteriol* **192:** 1020–1029.

Wahjudi, M., Papaioannou, E., Hendrawati, O., van Assen, A.H., van Merkerk, R., Cool, R.H., *et al.* (2011) PA0305 of *Pseudomonas aeruginosa* is a quorum quenching acylhomoserine lactone acylase belonging to the Ntn hydrolase superfamily. *Microbiology* **157:** 2042–2055.

Wang, L.H., He, Y., Gao, Y., Wu, J.E., Dong, Y.H., He, C., *et al.* (2004) A bacterial cell-cell communication signal with cross-kingdom structural analogues. *Mol Microbiol* **51:** 903–912.

Wang, Y., Cen, X.F., Zhao, G.P., and Wang, J. (2012) Characterization of a new GlnR binding box in the promoter of *amtB* in *Streptomyces coelicolor* inferred a PhoP/GlnR competitive binding mechanism for transcriptional regulation of *amtB. J Bacteriol* **194:** 5237–5244.

Weimar, J.D., DiRusso, C.C., Delio, R., and Black, P.N. (2002) Functional role of fatty acyl-coenzyme A synthetase in the transmembrane movement and activation of exogenous long-chain fatty acids. Amino acid residues within the ATP/AMP signature motif of *Escherichia coli* FadD are required for enzyme activity and fatty acid transport. *J Biol Chem* **277:** 29369–29376.

Yong, Y.C., and Zhong, J.J. (2013) Impacts of quorum sensing on microbial metabolism and human health. *Adv Biochem Eng Biotechnol* **131:** 25–61.

Zhang, H.B., Wang, L.H., and Zhang, L.H. (2002) Genetic control of quorum-sensing signal turnover in *Agrobacterium tumefaciens. Proc Natl Acad Sci USA* **99:** 4638–4643.

Supporting information

Additional Supporting Information may be found in the online version of this article at the publisher's web-site:

Fig. S1. Quantitative assay of DSF and BDSF levels in the supernatant of Xcc cultures using liquid chromatography-mass spectrometry (LC-MS).
Fig. S2. Time-course of growth, DSF and BDSF production in *Xcc* strains derived from the strain Δ*rpfC*.
Fig. S3. Quantitative assay of oleic acid level in the supernatant of *Xcc* cultures using gas chromatography-mass spectrometry (GC-MS).
Fig. S4. *In vitro* measurement of FCL activity of RpfB on DSF and BDSF.